

NON-INVASIVE BEAM DETECTION IN A HIGH-AVERAGE POWER ELECTRON ACCELERATOR

J. Williams, S. Biedron, J. Harris, J. Martinez, S. V. Milton, J. VanKeuren
 Electrical and Computer Engineering, Colorado State University, Fort Collins, Colorado
 S. V. Benson, P. Evtushenko, G. R. Neil, S. Zhang
 Jefferson National Lab, Newport News, Virginia

Abstract

For a free-electron laser (FEL) to work effectively the electron beam quality must meet exceptional standards. In the case of an FEL operating at infrared wavelengths the critical phase space tends to be in the longitudinal direction. Achieving high enough longitudinal phase space density directly from the electron injector system in an FEL is difficult due to space charge effects, thus one needs to manipulate the longitudinal phase space once the beam energy reaches a sufficiently high value. However, this is fraught with problems. Longitudinal space charge and coherent synchrotron radiation can both disrupt the overall phase space, furthermore, the phase space disruption is exacerbated by the longitudinal phase space manipulation process required to achieve high peak current. To achieve and maintain good FEL performance one needs to investigate the longitudinal emittance and be able to measure it during operation preferably in a non-invasive manner. Using electro-optical (EO) methods, we plan to measure the bunch longitudinal profile of an energy (~120-MeV), high-power (~10kW or more average FEL output power) beam. Such a diagnostic could be critical in efforts to diagnose and help mitigate deleterious beam effects for high output power FELs.

INTRODUCTION

In order to operate an FEL of high quality, an electron beam with high-peak current, low transverse emittance and low energy spread is required. An operational understanding of electron bunch parameters through diagnostics is needed if one wishes to achieve the optimal desired beam qualities. There are a number of diagnostics of both invasive and non-invasive genres used to determine electron bunch parameters. Invasive diagnostics such as transition radiation (CTR) screens placed directly into the beam of electrons are great if one has a low power beam and does not care if operation is momentarily interrupted. Such diagnostics are not suitable for high power operation as they will be destroyed by the beam, or operational monitoring as they severely disrupt the beam properties upon impact with the diagnostic. As an FEL requires high longitudinal phase space density for optimal output, the required manipulations of the electron bunches can lend to undesirable additional effects which need to be monitored in-situ, and, if possible, avoided. One needs a non-invasive longitudinal phase space diagnostic to allow for the achievement and maintenance of the beam properties.

A method to sample the bunch's electric field without prohibitively disrupting the beam is to utilize a crystal with a birefringent property influenced by an electric field, known as the electro-optical (EO) method. This property is caused by the Pockel's effect and the crystal acts as a Pockel's Cell driven by the electric fields of the electron bunches. The different polarizations of light within a pulse traversing the crystal will have altered path lengths created by the birefringence. The altered pulse becomes elliptically polarized in a manner proportional to the influence of induced birefringence. Equation (1) (derived in Jamison, et al. [1]), gives the resultant Fourier transform of the electron beam's Coulomb field with a probing optical pulse, and the resultant inverse transform in Equation (2). The functions $R(t)$ and $R(\omega)$ are the response of the crystal due its nonlinearity and phase matching.

$$E_{out}^{opt}(\omega) = E_{in}^{opt}(\omega) + i\omega E_{in}^{opt}(\omega) * [E^{Coul}(\omega)R(\omega)], (1)$$

$$E_{out}^{opt}(t) = E_{in}^{opt}(t) + a[E^{Coul}(t) * R(t)] \frac{d}{dt} E_{in}^{opt}(t). (2)$$

The Coulomb field becomes encoded in the optical pulse to later be processed in order to determine the longitudinal bunch profile.

For a relativistic electron, the radial Coulomb field is oriented perpendicular to propagation with an opening angle $\propto 1/\gamma^2$, where γ is the relativistic Lorentz factor. The strength of the field is a function of electron bunch distance, b , from the crystal as found in Eqn (3) below. This field is found to have an effect similar to radiation in the Terahertz region of the electromagnetic spectrum (~100-900 μ m wavelengths) [2]. Placing the desired (EO) crystal near the longitudinally propagating bunch charge encodes the electric field information in the crystal without directly altering the bunch. The induced birefringence is probed and encoded within an optical pulse incident normally on the crystal.

$$E_{y=b} = \frac{e}{4\pi\epsilon_0} \frac{\gamma b}{(b^2 + \gamma^2 z^2)^{3/2}} (3)$$

The facilities where EO diagnostics have been implemented are in contrast to the CSU and JLab accelerators, typically feature beamline parameters with short bunches, low average power and high electron beam energies. As an example, one facility that has employed an EOS diagnostic is FERMI@Elettra [3], which features a bunch length of ~.54 ps FWHM, operational beam

energy of 1.2 GeV, but at a much lower average power (10s of Watts). These differences in parameters, particularly the electron beam energy and average beam power, lead to modification of previous designs to suit our conditions.

METHODS

There are a variety of EO techniques utilized by different accelerator facilities, chosen based on their intrinsic strengths and weaknesses. It was shown at FELIX [4] that a scanning-delay method employed was capable of sub-picosecond measurements of longitudinal beam profile. In this diagnostic an initially linearly polarized 12-fs, 800-nm Ti:sapphire laser incident upon a ZnTe EO crystal placed near (6 mm from the bunch center) an electron pulse train is induced to elliptical polarization. The signal is further refined via use of a quarter wave plate and subsequent Wollaston prism to separate the polarization affected beam and the reference beam through a balance detector. Because the delay between the laser and the bunch train is scanned, this technique is subject to the natural laser pulse train jitter with respect to the beam and smearing of the resultant profile limiting the resolution further due to averaging of the signal over many pulses.

Another technique, known as spectral decoding, uses a chirped laser pulse to create a time-frequency relationship between the laser spectrum and the traversing electron bunch. This technique has been demonstrated at a number of facilities (FELIX, NSLS and FLASH [5-7]); however, there is a bunch length resolution limit, τ_{lim} , created by temporal distortion of the chirped pulse given by $\tau_{lim} = 2.6\sqrt{T_C T_0}$ [1], where T_C is the duration of the pulse generated by the electron beam and T_0 is that of the optical pulse length. A bunch length shorter than the resolution limit will distort the pulse signal due to Fourier transform artifacts [8]. An advantage of this method is that it is a single shot and so timing jitters and averaging of the signal do not affect resolution.

Similar to the previous method, another technique decodes the temporal profile of the electron bunch electrical field and is aptly known as temporal decoding. Using cross-correlation through second harmonic generation of the probe pulse that has been modified by the beam's electric field within the EO crystal, with a reference pulse (both split from a single pulse prior to probing of the crystal), a spatial mapping of the temporal intensity is created. This measurement is done in a single shot giving rise to individual bunch measurements. The FELIX facility has used this method to measure pulses with sub picosecond resolution [2,9]. A schematic of this method is given in Figure 1.

A fourth EO technique that differs in the manner of EO crystal probing is known as spatial encoding. Rather than probe the crystal with a laser pulse normal to the surface, a pulse broadened by a cylindrical telescope travels at an angle such that an encoding of the temporal profile of the Coulomb field is achieved across the transverse direction

of the pulse. The spatial signal is now a measure of the temporal changes of the Coulomb field. As seen in Figure 2, the electron beam still propagates normal to the EO crystal. Because the probe is broadened, any anisotropy of the birefringence may lead to signal errors and quality measurements rely on ideal EO crystals. Employed at SLAC [10,11] and DESY, this single-shot measurement is shown to be capable of <300 fs FWHM bunch length measurements.

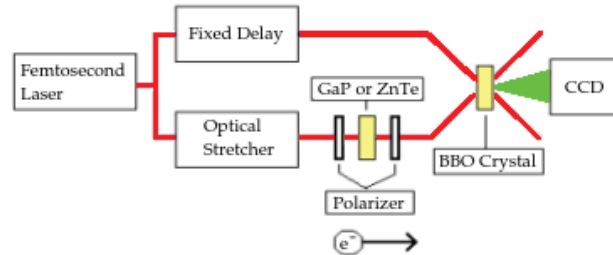


Figure 1: Electro-optical temporal decoding: A pulse is split such that a reference pulse travels through a fixed delay to be later combined the EO probe pulse in a non-linear crystal to create a pulse shape through Second Harmonic Generation (SHG).

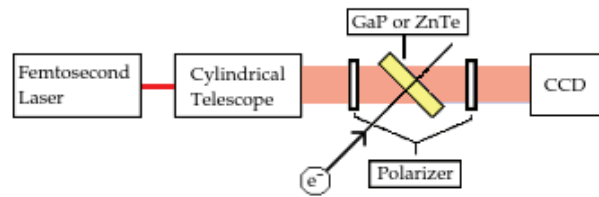


Figure 2: Diagram of electro-optical spatial encoding technique. Electron bunch still passes normal of the crystal, however, the probe pulse is incident obliquely. A cylindrical telescope is used to increase optical pulse transverse dimensions.

When designing the appropriate diagnostic to be implemented at CSU and Jefferson Lab, considerations of accuracy and effective measurement led us to choose the latter two introduced methods: EO temporal decoding and EO spatial encoding. Both of these are carried out in single-shot measurements allowing for single bunch signal probing. The spatial encoding method was found to be a relatively cheap option with a simple design. Where spatial encoding is limited in temporal resolution and noise susceptibility, temporal decoding compensates for these problems by providing excellent temporal resolution and low noise susceptibility due to the more complex cross-correlation design.

The beam energy for application at CSU, as well as the injection energy for the JLab accelerator, are both around 6 MeV. The beam energy for the second desired diagnostic location at Jefferson Lab is over 100 MeV and has a sub-picosecond bunch length. Based on Equation 3, there is a definite Coulomb field signal strength relation to distance from the beamline (b) which will have to be considered for our various applications. Clearly, placing an EO material further from the beamline is acceptable

for higher energies and desirable to mitigate crystal damage, and therefore the crystal holder will be designed accordingly.

Prior to beam line implementation, a THz generation kit from Newport [12] will be used to simulate the desired diagnostic situation. The kit produces a THz wave through AC-biased plasma collapse, which is made to co-propagate with a reference pulse through a ZnTe crystal. Emulation of a real electron beam will be enhanced in the future to more accurately recreate the perpendicularly propagating Coulomb field of an electron bunch passing near the crystal.

ELECTRO-OPTICAL CRYSTAL DEPENDENCE

In order to determine the ideal EO crystal to be used for an actual diagnostic, considerations of crystal damage threshold, resonance and effective radiation birefringence will be made pertinent to our beam conditions. Figures 3 and 4 show the expected electric field intensity and resolution limits for energies around 6 MeV, which is our design beam energy. It is clear that the longitudinal resolution time will be limited to picoseconds measurements, and the low expected intensity may require us to place the crystal in close proximity to the passing bunch (<5mm), possibly subjecting the crystal to heavy radiation and beam halo damage.

DEVELOPMENT AND IMPLEMENTATION

Prior to implementation of an EO system within the CSU and JLab beamlines, several steps must be taken. Initially, we must study how our high average power beams will affect various EO crystals.

After deciding on the optimal crystal, the EO techniques must be developed on a setup that is a physical realization of the apparatus to be installed on the beamline. Currently the THz kit is being assembled. This kit will be bench tested to confirm functionality of the parts and then it will be modified for single shot capability so that a single bunch measurement can be made. Additional modifications will be made to accommodate radiation pulses similar to those generated by the CSU electron beam.

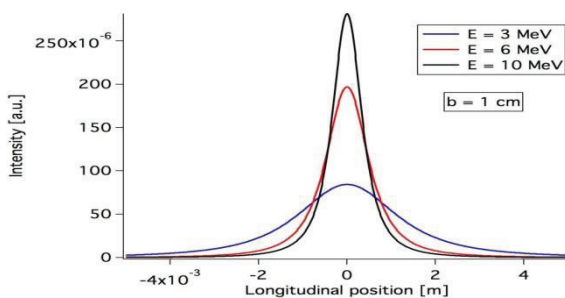


Figure 3: This figure shows the relative intensity of electron bunch electric field as a function of beam energy and position.

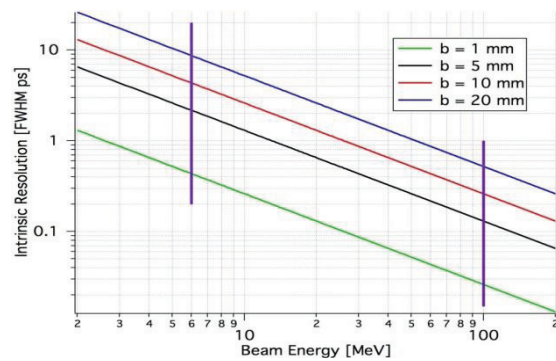


Figure 4: The time resolution of electron bunch EO signal is shown for various crystal distances and beam energies. The vertical bars mark the energies to be explored at CSU and JLab.

REFERENCES

- [1] S.P. Jamison et al., "Femtosecond Resolution Bunch Profile Measurements," Proc. of EPAC'06, Edinburgh, Scotland, TUYP01, p. 915 (2006); <http://www.JACoW.org>
- [2] G. Berden et al., Phys. Rev. Lett. 93 (2004) 11.
- [3] M. Veronese et al., "First Operation of the Electro Optical Sampling Diagnostics of the FERMI@ELETTRA FEL," IBIC'12, Tsukuba, Japan, TUPA43, p. 449 (2012); <http://www.JACoW.org>
- [4] X. Yan et al., Phys. Rev. Lett. 85 (2000) 16.
- [5] I. Wilke et al., Phys. Rev. Lett. 88 (2004) 12.
- [6] H. Loos et al., "Electro-optic Longitudinal Electron Beam Diagnostic at SDL," Proc. of PAC'03, WPPB021, p. 2455 (2003); <http://www.JACoW.org>
- [7] B. Steffen et al., "Spectral Decoding Electro Optic Bunch Length and Arrival Time Jitter Measurements at the DESY VUV-FEL," FEL'05, Palo Alto, CA, THPP039, p. 549 (2005); <http://www.JACoW.org>
- [8] B. Steffen and S. Casalbuoni et al., "Electro Optic Bunch Length Measurements at the VUV-FEL at DESY," Proc. of PAC'05, Knoxville, TN, RPAT080, p. 3111 (2005); <http://www.JACoW.org>
- [9] G. Berden et al., Phys. Rev. Lett. 99 (2007) 11.
- [10] A. L. Cavalieri et al., Phys. Rev. Lett. 94 (2005) 11.
- [11] H. Schlarb et al., "Comparative Study of Bunch Length and Arrival Time Measurements at FLASH," EPAC'06, Edinburgh, Scotland, TUPCH024, p.1049 (2006); <http://www.JACoW.org>
- [12] Newport Corporation, "Application Note 44: Terahertz Spectrometer based on Generation of Ultrafast Terahertz Pulses in Air Plasma," (2011).